# INTEGRATION OF SOLAR AND PV BATTERY WITH ADVANCED CONTROL STRATEGY OF A THREE-LEVEL NPC INVERTER

**[1]N CHANDRAMOHAN, [2]Y.NARASIMHA RAO**
[1]Mtech, NALANDA INSTITUTE OF ENGINEERING & TECHNOLOGY
[2]Associate Professor, NALANDA INSTITUTE OF ENGINEERING & TECHNOLOGY

**Abstract- In this paper proposes the design and analysis of the proposed configuration and the theoretical framework of the propose modulation technique. A novel configuration of a three-level neutral-point-clamped (NPC) inverter that can integrate solar photovoltaic (PV) with battery storage in a grid-connected system proposed in this paper. The strength of the proposed topology lies in a novel extended unbalance three-level vector modulation technique than can generate the correct ac voltage under unbalanced dc voltage conditions. In order to control the power deliver between the solar PV, battery, and grid, which simultaneously provides maximum power point tracking (MPPT) operation for the solar PV with new control algorithm for the proposed system is also presented. The effectiveness of the proposed methodology is investigated by the simulation of several scenarios, including battery charging and discharging with different levels of solar irradiation. By using the simulation results we can analyze the proposed method.**
**Index Terms—Battery storage, solar photovoltaic (PV), space vector modulation (SVM), three-level inverter**.

## I. INTRODUCTION

The power delivered by a PV system of one or more photovoltaic cells is dependent on the irradiance, temperature, and the current drawn from the cells. Maximum Power Point Tracking (MPPT) is used to obtain the maximum power from these systems. In solar PV or wind energy applications, utilizing maximum power from the source is one of the most important functions of the power electronic systems [3]–[5]. In three-phase applications, two types of power electronic configurations are commonly used to transfer power from the renewable energy resource to the grid: single-stage and double-stage conversion. In the double-stage conversion for a PV system, the first stage is usually a dc/dc converter and the second stage is a dc/ac inverter. The function of the dc/dc converter is to facilitate the maximum power point tracking (MPPT) of the PV array and to produce the appropriate dc voltage for the dc/ac inverter. The function of the inverter is to generate three-phase sinusoidal voltages or currents to transfer the power to the grid in a grid-connected solar PV system or to the load in a stand-alone system [3]–[5].

In the single-stage connection, only one converter is needed to fulfill the double-stage functions, and hence the system will have a lower cost and higher efficiency, however, a more complex control method will be required. This paper is concerned with the design and study of a grid-connected three-phase solar PV system integrated with battery storage using only one three-level converter having the capability of MPPT and ac-side current control, and also the ability of controlling the battery charging and discharging.

One of the main ideas of this paper is to have an overall view of the switching effects on a three-wire connection of a three-level NPC inverter with a combination of these systems on the dc side. This also can increase the flexibility of power system control and raise the overall availability of the system [2]. Usually, a converter is required to control the charging and discharging of the battery storage system and another converter is required for dc/ac power conversion; thus, a three phase PV system connected to battery storage will require two converters.

## II. STRUCTURE OF A THREE-LEVEL INVERTER AND ITS CAPACITOR VOLTAGE CONSIDERATIONS

### A. Three-Level Inverter

Fig. 1(a) shows a typical three phase three-level neutral-point-clamped (NPC) inverter circuit topology. The converter has two capacitors in the dc side to produce the three-level ac-side phase voltages. The capacitor voltages are assumed to be balanced, since it has been reported that unbalance capacitor voltages can affect the ac side voltages and can produce unexpected behavior on system parameters such as even-harmonic injection and power ripple.

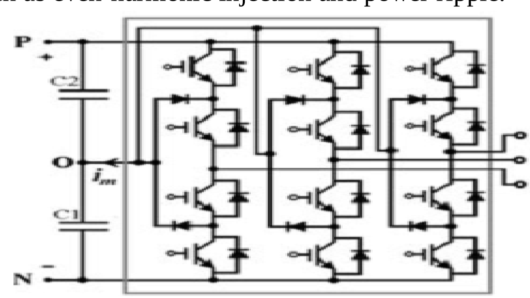


(a)

Fig. 1. Typical three-level inverter (a) structure of circuit,

### B. Balanced Capacitors Voltage

Various strategies have been proposed to balance the capacitor voltages using modulation algorithms such as sinusoidal carrier based PWM (SPWM) or space vector pulse width modulation (SVPWM). In SPWM applications, most of the strategies are based on injecting the appropriate zero-sequence signal into the modulation signals to balance the dc-link capacitors. In SVPWM applications, a better understanding of the effects of the switching options on the capacitor voltages in the vector space has resulted in many strategies proposed to balance capacitors voltages in the three-level NPC inverter. In any space vector modulation (SVM) scheme such as SVPWM and VSVPWM, the reference vector Vref is generated by selecting the appropriate available vectors in each time frame in such a way that the average of the applied vectors must be equal to the reference vector. Equation (1) shows the mathematical relation between the timing of the applied vectors and the reference vector

$$\begin{cases} T_s\vec{V}_{ref} = \sum_{i=1}^{n} T_i\vec{V}_i \\ T_s = \sum_{i=1}^{n} T_i \end{cases} \quad (1)$$

Where Ts is the time frame and preferred to be as short as possible. Ti is the corresponding time segment for selected inverter vector Vi and n is the number of applied vectors.

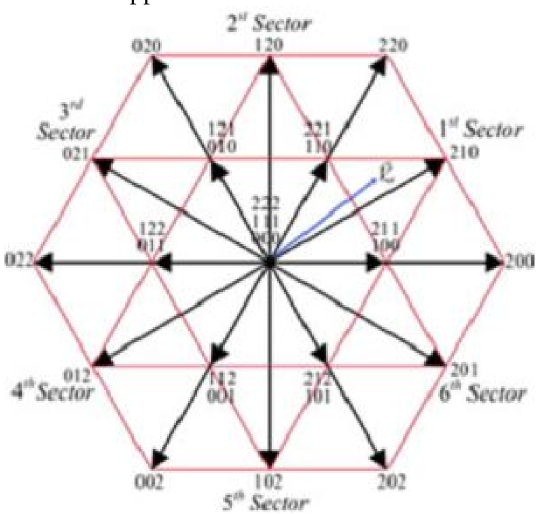


(b)

Fig. 1. Typical three-level inverter (b) three-level inverter space vector diagram for balanced dc-link capacitors

Fig. 1(b) shows the space vector diagram of a three-level inverter for balanced dc-link capacitors [6]. It is made up of 27 switching states, from which 19 different voltage vectors can be selected. The number associated with each vector in Fig. 1(b) represents the switching state of the inverter phases respectively. The voltage vectors can be categorized into five groups, in relation to their amplitudes and their effects on different capacitor voltages from the view of the inverter ac side. They are six long vectors (200, 220, 020, 022, 002, and 202), three zero vectors (000, 111, and 222), six medium vectors (210, 120, 021, 012, 102, and 201), six upper short vectors (211, 221, 121, 122, 112, and 212), and six lower short vectors (100, 110, 010, 011, 001, and 101). For generating Vref, when one of the selections( Vi), is a short vector, then there are two choices that can be made which can produce exactly the same effect on the ac side of the inverter in the three wire connection (if voltages are balanced). For example, the short vector “211” will have the same effect as “100” on the ac side of the inverter.

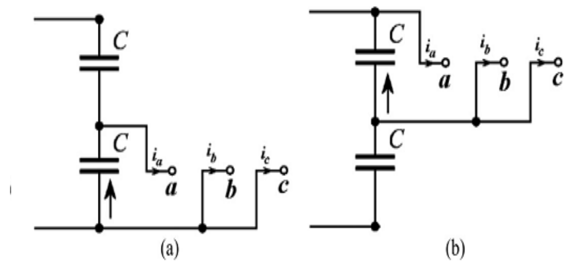


Fig. 2. Equivalent circuit and capacitors current with two different short vector.
(a)Short vector—100. (b) Short vector—211.

For example, Fig. 2 shows the connection of the capacitors when “100”or “211” is selected, demonstrating how different capacitors are involved in the transfer of power. Capacitor balancing in most reported three-level NPC inverter applications is achieved by the proper selection of the short vectors.

### C. Unbalanced Capacitor Voltages

Fig. 3 shows a general structure of a grid-connected threelevel inverter showing the dc and ac sides of the inverter. The dc-side system, shown as “N” can be made up of many circuit configurations, depending on the application of the inverter. For instance, the dc-side system can be a solar PV, a wind generator with a rectifying circuit, a battery storage system or a combination of these systems where the dc voltage across each capacitor can be different or equal.

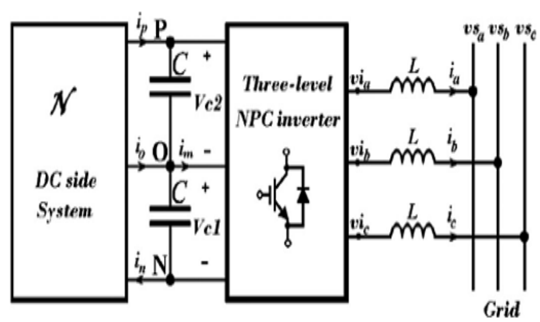


Fig. 3. General diagram of a grid connected three-wire three-level inverter.

Mathematically, in a three-wire connection of a two-level inverter, the dq0field,vd,vq, and v0 of the inverter in vector control can be considered as having two degrees of freedom in the control system; because the zero sequence voltage, v0 will have no effect on the system behavior in both the dc and the ac side of the inverter. However, in the three-level three-wire application illustrated in Fig. 3, with fixed vdandvq althoughv0 will have no effect on the ac-side behavior, it can be useful to take advantage ofv0to provide a new degree of freedom to control the sharing of the capacitor voltages in the dc bus of the inverter.

**D. Effect of Unbalanced Capacitor Voltages**

on the Vector Diagram In the vector diagram shown in Fig. 1(b), capacitor voltage unbalance causes the short and medium vectors to have different magnitudes and angles compared to the case when the capacitor voltages are balanced.

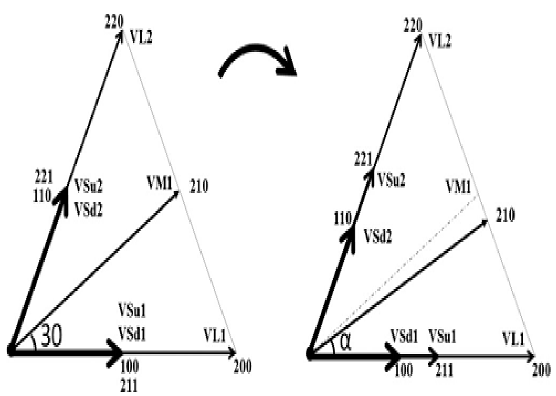


Fig. 4. Vector diagram in the first sector of Fig. 1(b) showing the change ofthe vectors using balanced dc and unbalanced dc assumingVc1<Vc2

Fig. 4 shows the differences between two cases as highlighted in the first sector of the sextant in Fig. 1(b) forVC1 <VC2.Vector related to the switching stateVI can be calculated as follows [20]:

$$\vec{V}_I = \frac{2}{3}(V_{aN} + \vec{a}V_{bN} + \vec{a}^2V_{cN}) \qquad (2)$$

wherea=ej(2π 3 ) andVaN,VbN andVcN are the voltage values of each phase with reference to "N" in Fig. 1(a). Assuming that the length of the long vectors ((2/3)Vdc) is 1 unit and the voltage of capacitorC1,Vc1 =hV dc,for0≤h≤1, then the vectors in the first sector can be calculated using (2) and the results are given in (3)–(9)

$$\vec{V}sd1 = h \qquad (3)$$

$$\vec{V}su1 = 1 - h \qquad (4)$$

$$\vec{V}l1 = 1 \qquad (5)$$

$$\vec{V}l2 = \frac{1}{2} + \frac{\sqrt{3}}{2}j \qquad (6)$$

$$\vec{V}sd1 = h\left(\frac{1}{2} + \frac{\sqrt{3}}{2}j\right) \qquad (7)$$

$$\vec{V}su2 = (1-h)\left(\frac{1}{2} + \frac{\sqrt{3}}{2}j\right) \qquad (8)$$

$$\vec{V}m1 = \left(1 - \frac{h}{2}\right) + h\frac{\sqrt{3}}{2}j \qquad (9)$$

The vectors in the other sectors can be calculated similarly. Equations (3)–(9) show that the magnitudes and the angles of the vectors can change depending on the value of the capacitor voltages.

**E. SELECTING VECTORS UNDER UNBALANCED DC VOLTAGE CONDITION AND THEIR EFFECTS ON THE AC SIDE OF INVERTER**

To generate a reference vector based on (1), different combinations can be implemented. Fig. 5 shows different possible vector selections to generate a reference vector( V ∗ )in the first sector based on the selections of different short vectors.

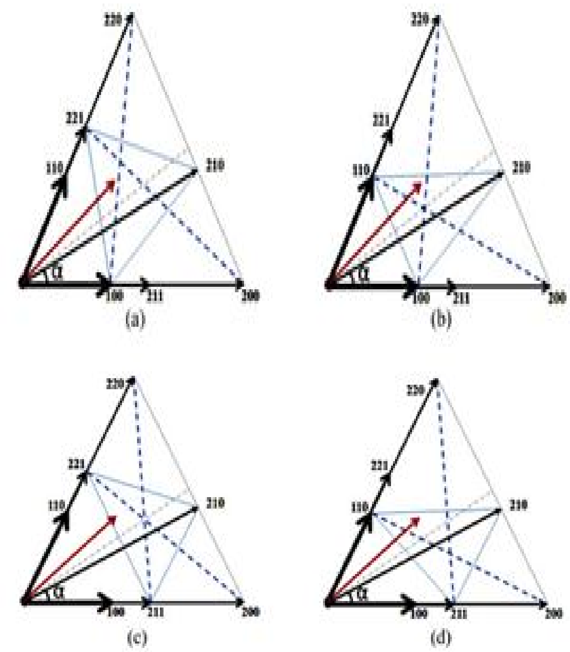


Fig. 5. Different possible vector selection ideas

For example, to generate V ∗ based on Fig. 5(a), one of following combinations can be selected with proper timing based on (1). The combinations are: (221–210–100), (221–220–100), (221– 200–100), (221–200–Zero), (000–220–Zero), (220–200–Zero), where "Zero" can be "000" or "111" or "222". This demonstrates that there is flexibility in choosing the correct vector selections.

To investigate the continuous time behavior of the ac-side voltages, the error vectore(t) can be calculated in order to determine how far the generated voltage deviates from the requested vector as follows:

$$\vec{e}(t) = \vec{V}^*(t) - \vec{V}_{apl}(t) \qquad (10)$$

$$E(t) \triangleq \left|\int_0^t \vec{e}(t)dt\right|; \;\; 0 \le t \le T_s \qquad (11)$$

where Vapl(t)is the applied vector at the time "t". This error can result in harmonic current across the impedance connected between the inverter and the grid. If this impedance is an inductor then the ripple in the inductors current IrLcan be expressed as

$$\vec{I}_{rL} = {}^{1}/_{L} \int_0^t \vec{e}(t)dt \quad (12)$$

Where e(t)is defined as

$$\vec{e}(t) \triangleq L\frac{d\vec{I}_{rL}}{dt} \quad (13)$$

To derive (13), it is assumed that the requested vectorV ∗ (t) will generate sinusoidal current in the inductor, which is normally acceptable in the continuous time behavior of the system.

**F. Selecting Vectors Under Unbalanced DC Voltage**

Conditions and Their Effects on DC Side of the Inverter As far as the dc side is concerned, different vectors have different effects on the capacitor voltages which depend on the sum of the incoming currents from the dc side and the inverter side.

The instantaneous power transmitted to the dc side of the inverter from the ac side can be calculated as follows:

$$p(t) = v_{Ia}.i_a + v_{Ib}.i_b + v_{Ic}.i_c \quad (14)$$

Where vIa, vIb, and vIc are the ac-side inverter instantaneous voltages with reference to the "N" point, and ia, ib, ic are inverter currents. For example, in the first sector of the vector diagram shown in Fig. 4, p(t)for the short vectors can be expressed by the following equations:

$$\begin{cases} p_{211}(t) = (1-h)Vdc * i_a \\ p_{100}(t) = hVdc * (-i_a) \end{cases} \quad (15)$$

$$\begin{cases} p_{211}(t) = (1-h)Vdc * (-i_c) \\ p_{110}(t) = hVdc * i_c \end{cases} \quad (16)$$

Ignoring the dc-side system behavior, selecting the upper short vectors, "211" and "221," will affect the upper capacitor voltage, and selecting the lower short vectors, "100" and "110," will affect the lower capacitor voltage..

## III. PROPOSEDTOPOLOGY TOINTEGRATESOLARPVANDBATTERYSTORAGE ANDITSASSOCIATEDCONTROL

### A. Proposed Topology to Integrate Solar PV and Battery Storage Using an Improved Unbalanced DC Functionality of a Three-Level Inverter

Two new configurations of a three-level inverter to integrate battery storage and solar PV shown in Fig. 6 are proposed, where no extra converter is required to connect the battery storage to the grid connected PV system. These can reduce the cost and improve the overall efficiency of the whole system particularly for medium and high power applications. Fig. 6(a) shows the diagram of the basic configuration. In the proposed system, power can be transferred to the grid from the renewable energy source while allowing charging and discharging of the battery storage system as requested by the control system.

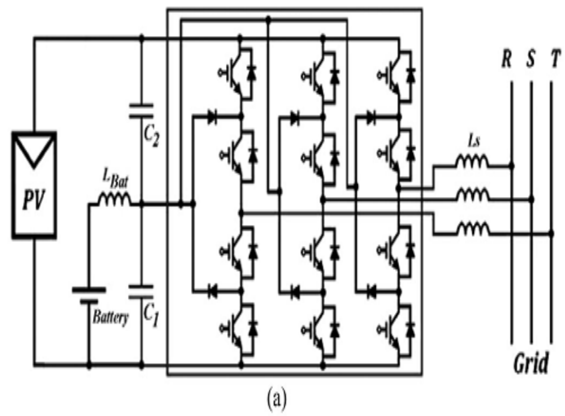


Fig. 6. Proposed configurations for integrating solar PV and battery storage: (a) basic configuration;

Fig. 6(b) shows the improved configuration where two batteries are now connected across two capacitors through two relays. When one of the relays is closed and the other relay is open, the configuration in Fig. 6(b) is similar to that in Fig. 6(a) which can charge or discharge the battery storage while the renewable energy source can generate power.

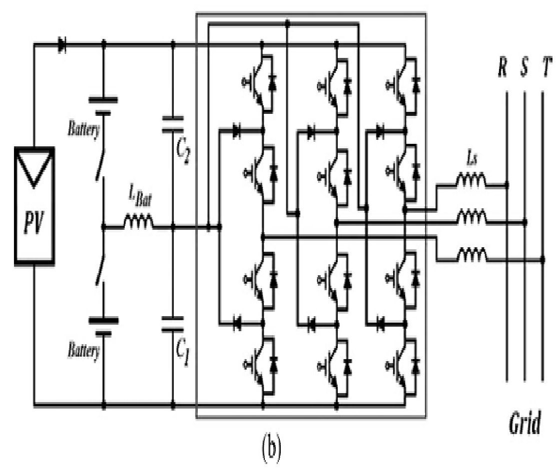


Fig. 6. Proposed configurations for integrating solar PV and battery storage: (a) basic configuration; (b) improved configuration.

However, when the renewable energy is unavailable, both relays can be closed allowing the dc bus to transfer or absorb active and reactive power to or from the grid. It should be noted that these relays are selected to be ON or OFF as required; there is no PWM control requirement. This also provides flexibility in managing which of the two batteries is to be charged when power is available from the renewable energy source or from the grid.

INTERNATIONAL JOURNAL OF RESEARCH
In Advanced Engineering Technologies
Volume 6, Issue 2 AUG 2017

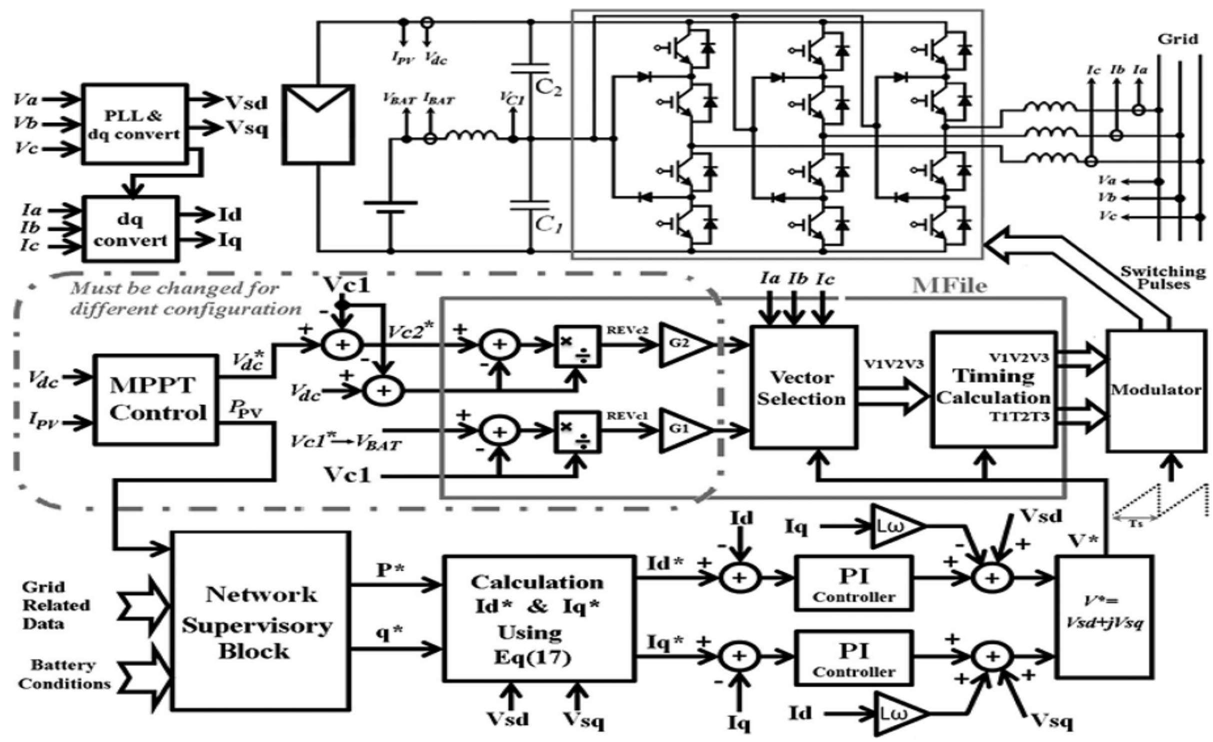


Fig. 7. Control system diagram to integrate PV and battery storage

## B. Control Topology

In Fig. 6(b), three different relay configurations can be obtained: 1) when the top relay is closed; 2) when the bottom relay is closed; and 3) when both relays are closed. Fig. 7 shows the block diagram of the control system for configuration 1). In Fig. 7, the requested active and reactive power generation by the inverter to be transferred to the grid will be determined by the network supervisory block. This will be achieved based on the available PV generation, the grid data, and the current battery variables.

The MPPT block determines the requested dc voltage across the PV to achieve the MPPT condition. This voltage can be determined by using another control loop, with slower dynamics,using the measurement of the available PV power. The details of the MPPT algorithm to determine the desired voltage(V ∗ dc ) can be found in [3] and [4]. Based on the requested active( ∗ )and reactive power(q ∗ ), and the grid voltage in thedq-axis,vsd andvsq, the requested inverter current in the dq-axis,id andiq can be obtained using (17):

$$\begin{cases} p = v_{sd}i_d + v_{sq}i_q \\ q = v_{sq}i_d + v_{sd}i_q \end{cases}$$

$$i_d^* = \frac{p^* v_{sd} - q^* v_{sq}}{v_{sd}^2 + v_{sq}^2}; \qquad i_q^* = \frac{q^* v_{sd} - p^* v_{sq}}{v_{sd}^2 + v_{sq}^2} \qquad (17)$$

By using a proportional and integral (PI) controller and decoupling control structure, the inverter requested voltage vector can be calculated. The proposed control system is shown in Fig. 7. In the proposed system, to transfer a specified amount of power to the grid, the battery will be charged using surplus energy from the PV or will be discharged to support the PV when the available energy cannot support the requested power.

To determine which short vectors are to be selected, the relative errors of capacitor voltages given in (18) and (19) are used

$$eV_{c1} = \frac{V_{C1}^* - V_{C1}}{V_{c1}} \qquad (18)$$

$$eV_{c2} = \frac{V_{C2}^* - V_{C2}}{V_{c2}} \qquad (19)$$

whereV ∗ C1 andV ∗ C2 are the desired capacitor voltages, andVC1 andVC2 are the actual capacitor voltages for capacitorC1 and C2, respectively.

The selection of the short vectors will determine which capacitor is to be charged or discharged. A decision function “F,” as given in (20), can be defined based on this idea

$$F = G_1 e_{Vc1} - G_2 e_{Vc2} \qquad (20)$$

Where G1 andG2 are the gains associated with each of the relative errors of the capacitor voltages. G1 andG2 are used to determine which relative error of the capacitor voltages is more important and consequently allows better control of the chosen capacitor voltage.

In each time step, the sign ofFis used to determine which short vectors are to be chosen. WhenFis positive, the short vectors need to be selected that can chargeC1 or dischargeC2 in that particular time step by applying (14) and using similar reasoning to (15) and (16). Similarly, whenFis negative, the short vectors need to be selected that can chargeC2or dischargeC1in that particular time step.

The same control system is applicable for configuration 2) by changing the generated reference voltages for the capacitors. Configuration 3) represents two storage systems connected to grid without any PV contribution, such as at night when the PV is not producing any output power.

## IV. SIMULATION ANDVALIDATION OF THE PROPOSED TOPOLOGY AND CONTROL SYSTEM

Simulations have been carried out using MATLAB/Simulink to verify the effectiveness of the proposed topology and control system. An LCL filter is used to connect the inverter to the grid. Fig. 8 shows the block diagram of the simulated system.

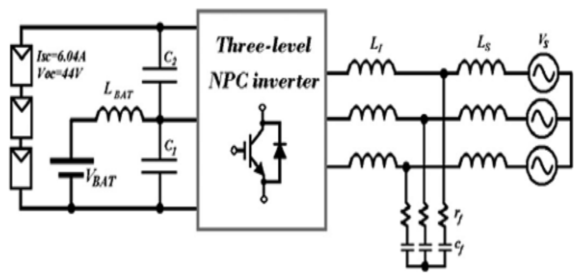


Fig. 8. Block diagram of the simulated system.

TABLE I
PARAMETERS OF THESIMULATEDSYSTEM

| $V_{BAT}$ | Vs (line) | $L_{BAT}$ | $C_1$,$C_2$ | $L_f$ | $L_S$ |
|---|---|---|---|---|---|
| 60 V | 50 V | 5 mH | 1000 uF | 500 uH | 900 uH |
| $r_f$ | $C_f$ | $K_p$ | $K_i$ | $G_1$ | $G_2$ |
| 3 Ω | 14 uF | 2.9 | 1700 | 1 | 200 |

Three, series-connected PV modules are used in the simulation. The mathematical model of each of the PV units is given in (21) [21] and used in the simulation

$$IPV = I_{SC} - 10^{-7}\left(e^{\left(\frac{V_{PV}}{2574*10^{-3}}\right)} - 1\right) \qquad (21)$$

Where ISC is the short circuit current of the PV.

For theoretical purposes, two different scenarios have been simulated to investigate the effectiveness of the proposed topology and the control algorithm using a step change in the reference inputs under the following conditions:

1) The effect of a step change in the requested active and reactive power to be transferred to the grid when the solar irradiance is assumed to be constant.

2) The effect of a step change of the solar irradiation when the requested active and reactive power to be transmitted to the grid is assumed to be constant.

### A. First Theoretical Scenario

Fig. 9 shows the results of the first scenario simulation. The simulation results in Fig. 9 show that the whole system produces a very good dynamic response. Fig. 10 shows the inverter waveforms for the same scenario.

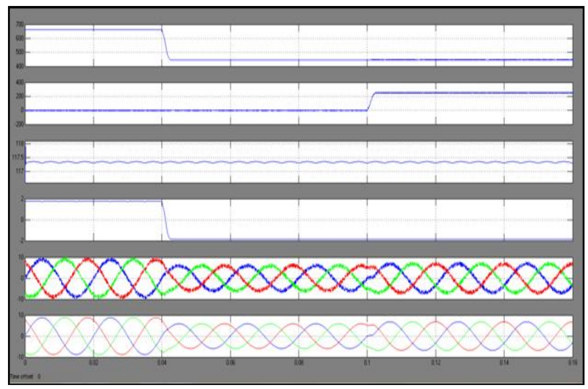

Fig. 9. Simulated results for the first scenario. (a) Active power injected to the grid. (b) Reactive power injected to the grid. (c) PV module DC voltage. (d) Battery current. (e) Inverter AC current. (f) Grid current.

Fig. 10(a) shows the line-to-line voltage Vab, and Fig. 10(b) shows the phase to midpoint voltage of the inverter Vao. Fig. 10(c) and (e) shows Vao,Von, and Van after mathematical filtering to determine the average value of the PWM waveforms

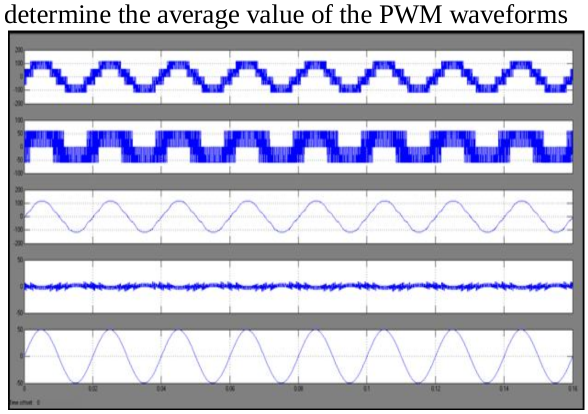

Fig. 10. Simulated inverter waveforms. (a) Vab-Phase to phase inverter voltage. (b) Vao-Inverter phase voltage reference to midpoint. (c) Filtered Von Filtered inverter phase voltage reference to midpoint.

(d) Filtered Von-Filtered midpoint voltage reference to neutral. (e) Filtered Van-Filtered phase voltage reference to neutral.

**B. Second Theoretical Scenario**

Fig. 11 shows the results of the second scenario simulation. Fig. 11(a) shows that the inverter is able to generate the requested active power. Fig. 11(b) shows that the PV voltage was controlled accurately for different solar irradiation values to obtain the relevant maximum power from the PV modules.

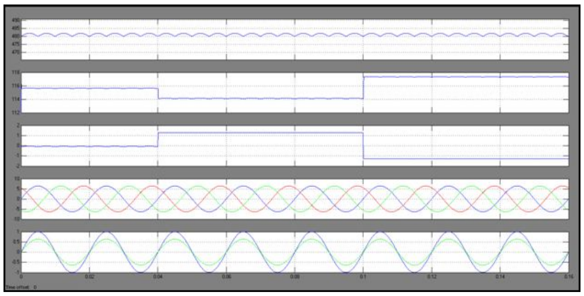

Fig. 11. Simulated results for the second scenario. (a) Active power injected to the grid. (b) PV module DC voltage. (c) Battery currents. (d) Grid side currents. (e) Grid side Phase (a) voltage and its current.

**C. Practically Oriented Simulation**

Fig. 12(a) shows that the active power transmitted to the grid reduces and follows the requested active power. Fig. 12(c) shows the ac inverter currents slowly decreasing starting from 3.4Arms att=40 ms and finally stays constant at 1.9Arms att=90 ms.

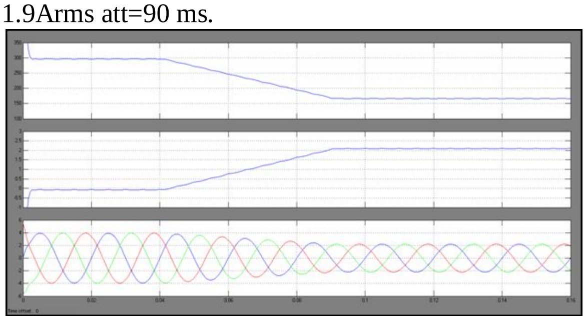

Fig. 12. Simulated result for third scenario. (a) Active power injected to the grid. (b) Battery current. (c) Grid side currents.

## VI. CONCLUSION

The main aim of this paper is to have an overall view of the switching effects on a three-wire connection of a three-level NPC inverter with a combination of these systems on the dc side. Grid connected renewable energy systems accompanied by battery energy storage can overcome this concern. This also can increase the flexibility of power system control and raise the overall availability of the system. In this paper proposes a novel topology for a three-level NPC voltage source inverter that can integrate both renewable energy and battery storage on the dc side of the inverter. A theoretical framework of a novel extended unbalance three-level vector modulation technique that can generate the correct ac voltage under unbalanced dc voltage conditions has been proposed. A new control algorithm for the proposed system has also been presented in order to control power flow between solar PV, battery, and grid system, while MPPT operation for the solar PV is achieved simultaneously. By using the simulation results we can control both PV and battery storage in supplying power to the ac grid.

## REFERENCES

[1] O. M. Toledo, D. O. Filho, and A. S. A. C. Diniz, “Distributed photovoltaic generation and energy storage systems: A review,”Renewable Sustainable Energy Rev., vol. 14, no. 1, pp. 506–511, 2010.

[2] M. Bragard, N. Soltau, S. Thomas, and R. W. De Doncker, “The balance of renewable sources and user demands in grids: Power electronics for modular battery energy storage systems,”IEEE Trans. Power Electron., vol. 25, no. 12, pp. 3049–3056, Dec. 2010.

[3] A. Yazdani and P. P. Dash, “A control methodology and characterization of dynamics for a photovoltaic (PV) system interfaced with a distribution network,”IEEE Trans. Power Del., vol. 24, no. 3, pp. 1538–1551, Jul.2009.

[4] A. Yazdani, A. R. Di Fazio, H. Ghoddami, M. Russo, M. Kazerani, J. Jatskevich, K. Strunz, S. Leva, and J. A. Martinez, “Modeling guidelines and a

benchmark for power system simulation studies of three-phase single-stage photovoltaic systems,"IEEE Trans. Power Del., vol. 26, no. 2, pp. 1247–1264, Apr. 2011.

[5] M. A. Abdullah, A. H. M. Yatim, C. W. Tan, and R. Saidur, "A review of maximum power point tracking algorithms for wind energy systems," Renewable Sustainable Energy Rev., vol. 16, no. 5, pp. 3220–3227, Jun. 2012.

[6] S. Burusteta, J. Pou, S. Ceballos, I. Marino, and J. A. Alzola, "Capacitor voltage balance limits in a multilevel-converter-based energy storage system," inProc. 14th Eur. Conf. Power Electron. Appl., Aug./Sep. 2011, pp. 1–9.

[7] L. Xinchun, Shan Gao, J. Li, H. Lei, and Y. Kang, "A new control strategyto balance neutral-point voltage in three-level NPC inverter," in Proc. IEEE 8th Int. Conf. Power Electron. ECCE Asia, May/Jun. 2011, pp. 2593–2597.

[8] J. Rodriguez, S. Bernet, P. K. Steimer, and I. E. Lizama, "A survey on neutral-point-clamped inverters,"IEEE Trans. Ind. Electron., vol. 57, no. 7, pp. 2219–2230, Jul. 2010.

[9] A. Lewicki, Z. Krzeminski, and H. Abu-Rub, "Space-vector pulsewidth modulation for three-level npc converter with the neutral point voltage control,"IEEE Trans. Ind. Electron., vol. 58, no. 11, pp. 5076–5086, Nov. 2011.